Available online at www.sciencedirect.com
ScienceDirect
Trans. Nonferrous Met. Soc. China 26(2016) 39−50
Transactions of Nonferrous Metals Society of China
www.tnmsc.cn

Microstructure evolution and segregation behavior of thixoformed Al−Cu−Mg−Mn alloy

Gang CHEN[1], Tao ZHOU[2], Bo WANG[3], Hong-wei LIU[1], Fei HAN[1]

1. School of Materials Science and Engineering, Harbin Institute of Technology, Weihai 264209, China;
2. Key Model Department, Air Force Equipment Department, Beijing 100081, China;
3. Beijing Spacecrafts, Beijing 100094, China

Received 23 January 2015; accepted 17 June 2015

Abstract: A commercial wrought Al−Cu−Mg−Mn alloy (2024) was thixoformed based on the recrystallization and partial melting (RAP) route, and the microstructure evolution and segregation behavior during the indirect thixoforming process were studied. The results show that fine spheroidal microstructures can be obtained by partial remelting of commercial extruded 2024 alloys without additional thermomechanical processing. During the indirect thixoforming, the stress distribution can be optimized by increasing the thickness of base region. Under three-dimensional compression stress state, the microstructures are homogeneous among different regions with no evidence of liquid segregation and micro-porosities, and the grains in the columns are deformed plastically. The distribution of tensile mechanical properties is consistent with the microstructures. Moreover, the distribution of deformation mechanism was discussed, and a technical method for improving the stress distribution was proposed.

Key words: aluminum alloy; semi-solid; thixoforming; segregation; microstructure

1 Introduction

Semi-solid processing (SSP) is a novel technology for forming alloys in the semi-solid state to near net shaped products. In comparison with conventional forming technologies, SSP has many advantages, such as lower forming force, less product defects and longer die life [1]. Thixoforming is a semi-solid metal processing route, which involves reheating suitable material into the semi-solid state and then forming it to near net shaped components [2−4]. The materials must have an appreciable melting range, and the microstructures must consist of solid metal spheroids in a liquid matrix before thixoforming [5−9]. Thixoforming can be classified into two types: direct forming and indirect forming [10,11]. For direct thixoforming, the semi-solid alloy is placed into opened dies and then deformed by the upper punch, and the deformation process is similar to open-die forging. The indirect thixoforming system consists of upper and lower dies and a punch, and the semi-solid alloy is forced into the previously closed dies and then deformed by the punch. The former type is suitable for forming components with simple or axial symmetric shapes, while the latter one could fabricate components with relatively complex shapes.

Thixoforming can provide high mechanical properties which are close to wrought target. Commercial thixoformed components are almost made from conventional casting alloys, which have high fluidity and castability [12−14]. However, the thixoforming of wrought aluminum alloys was limited due to some general difficulties which were summarized by LIU et al [15], such as wide freezing range (results in higher hot tearing sensitivity) and steep slope in liquid fraction versus temperature curves (leads to a small processing window). In recent years, increasing attention has been given to the thixoforming of wrought aluminum alloys, such as Al−Zn−Mg−Cu and Al−Cu−Mg series.

Some commercial wrought aluminum alloys are

Foundation item: Project (51405100) supported by the National Natural Science Foundation of China; Project (2014M551233) supported by the Postdoctoral Science Foundation of China; Project (HIT.NSRIF.2015112) supported by the Natural Scientific Research Innovation Foundation in Harbin Institute of Technology, China; Project (HIT(WH)201313) supported by the Scientific Research Foundation of Harbin Institute of Technology at Weihai, China

Corresponding author: Hong-wei LIU; Tel: +86-631-5687324; E-mail: liu_hongwei@hotmail.com

DOI: 10.1016/S1003-6326(16)64086-4

supplied in the extruded state. It is consistent with the recrystallization and partial melting (RAP) route, which involves warm working and partial remelting. During reheating, recrystallisation occurs in the extruded materials, and as liquid forms, it penetrates the recrystallised boundaries to form spheroids surrounded by liquid [16]. Therefore, it will be significant to obtain spheroidal microstructures directly from commercial extruded alloys without additional thermomechanical processing. JIANG et al [17] studied the microstructure evolution and coarsening by reheating the as-received 7005 aluminum alloy to the semi-solid state. They obtained spheroidal microstructures which are suitable for semi-solid processing. BIROL [18] studied the thixoformability of AA6082 aluminum alloy reheated from the as-cast and extruded states, respectively. KANG et al [10,19,20] have done much work on the microstructures and mechanical properties of thixoformed aluminum alloys.

Although many researches have been conducted on the thixoforming of wrought aluminum alloys and liquid segregation during semi-solid casting or rheoforming, little work has been done on the segregation behavior of indirectly thixoformed wrought aluminum alloys. The present work aims to study the segregation behavior of a thixoformed Al−Cu−Mg−Mn alloy. Moreover, the microstructure evolution and mechanical properties of the components thixoformed under different mechanical conditions were presented.

2 Experimental

The commercial wrought 2024 aluminum alloy was supplied by Northeast Light Alloy Co., Ltd., China, in the form of extruded rods with 45 mm in diameter with extrusion ratio of 1:17. The composition of the starting material is given in Table 1. Differential scanning calorimetry (DSC) was used to determine the solidification interval and the liquid fraction−temperature relationship. About 30 mg samples with 3 mm in diameter were heated to 700 °C at 10 °C/min and cooled to room temperature at the same rate. The change in liquid fraction with temperature was obtained from the heat flow versus temperature curve, as shown in Fig. 1.

Table 1 Composition of 2024 aluminum alloy (mass fraction, %)

Cu	Mg	Mn	Fe	Si	Ni	Zn	Ti	Al
3.8−4.9	1.2−1.8	0.3−0.9	0.5	0.5	0.10	0.30	0.15	Bal.

In order to investigate the microstructure evolution of the commercial wrought 2024 aluminum alloy during partial remelting, some samples with a diameter of 8 mm and a length of 12 mm were cut from the as-received rods. The samples were then reheated in an electrical resistance furnace into the semi-solid state, and isothermally held at 620 °C for different time and quenched in water to room temperature. A thermocouple was placed in a hole with 2 mm in diameter and 4 mm in depth in the center of the sample to ensure accurate temperature measurement and feedback control. According to the DSC results, the liquid fraction (φ_L) of 2024 alloy is 38.8 % at 620 °C.

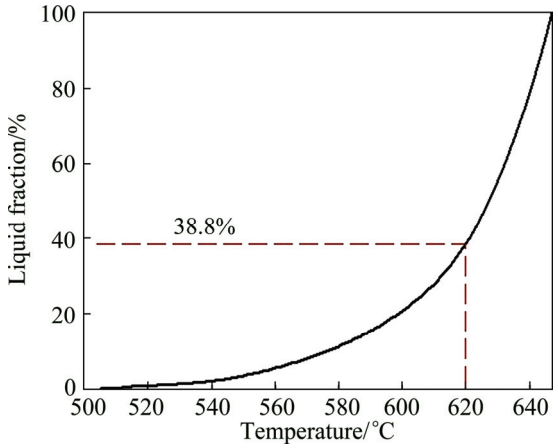

Fig. 1 Change in liquid fraction with temperature of 2024 aluminum alloy

A series of complex shaped components were designed and thixoformed. The components have four columns with different sizes in order to make distinct segregation during the thixoforming process. Figure 2 shows the schematic diagram of indirect thixoforming. As shown in Fig. 2(a), the indirect thixoforming dies consist of upper and lower dies and a punch. The four columns, from the largest one to the least one, are indicated as 1, 2, 3 and 4, respectively, and the base is indicated as 5.

The thixoforming process was carried out using a double-action hydraulic press, which could provide the maximum load of 5000 kN for locking the dies and 1000 kN for the punch. The as-received rods were machined to cylinder-shaped slugs with a diameter of 42 mm and heights of 48 and 56 mm, respectively, so as to thixoform the components with different base thicknesses (3 and 10 mm, respectively). The slugs were rapidly reheated to 620 °C using an electrical resistance furnace. The heating process was monitored by a K-type thermocouple, located at a depth of 10 mm from the top center of slug, which were quickly removed prior to actual thixoforming. During the thixoforming process, the pressure exerted on the slug was increased rapidly to a pre-determined level. The loading velocity and dwelling time were 150 mm/s and 30 s, respectively.

The thixoformed components were then subjected to standard heat treatment T6 (solution treatment at

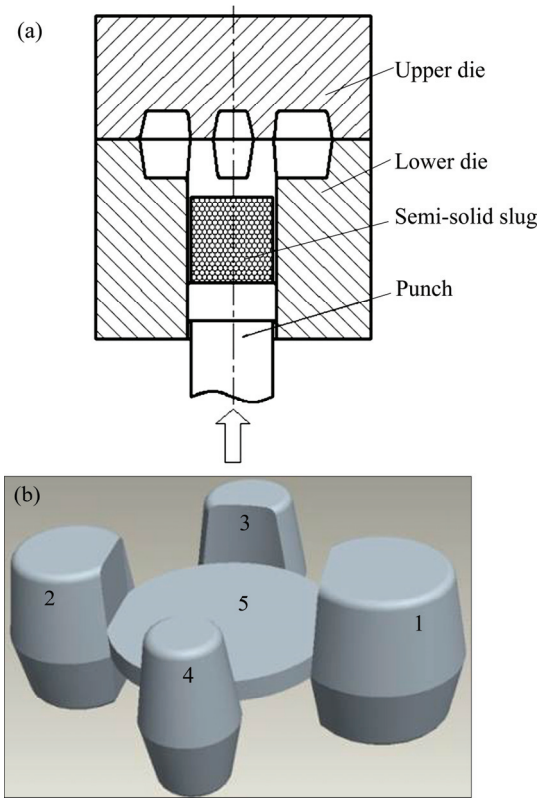

Fig. 2 Schematic diagram of indirect thixoforming (a) and thixoformed component (b)

490 °C for 2 h followed by water quenching and then aging at 190 °C for 10 h). The samples for microstructure examination and tensile tests were machined from different positions of the thixoformed parts. The microstructures were examined by optical microscopy (OM) and scanning electron microscopy (SEM) equipped with an energy dispersive X-ray spectrometer (EDS). The grain size (D= $(4A/\pi)^{1/2}$, where A is the area of solid grain) and shape factor (F=$4\pi A/P^2$, where P is the solid grain perimeter) were measured from the resulted microstructures using an image analysis system. The samples for OM and SEM were prepared by standard technique of grinding with SiC abrasive and polishing with a diamond spray (0.5 μm), and then etched with 2.5%HNO_3+1.5%HCl+1%HF aqueous solution for about 20 s. The tensile mechanical properties were measured using an INSTRON 5582 universal testing machine at a cross head speed of 1 mm/min. Each tensile value is the average of three measurements.

3 Results

3.1 Microstructure evolution of as-received alloy during partial remelting

Figure 3 shows the longitudinal section optical micrograph of as-received wrought 2024 aluminum alloy. As shown in Fig. 3, the microstructure consists of elongated and fibrous grains which are aligned to the extrusion direction, indicating that the alloy underwent severe plastic deformation and did not recrystallize. Therefore, the partial remelting of this material can be classified as being consistent with the RAP route.

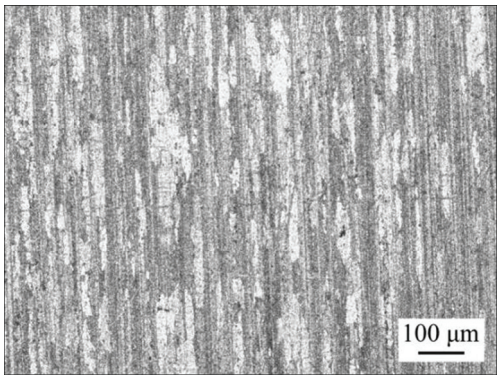

Fig. 3 Microstructure of as-received wrought 2024 aluminum alloy in longitudinal section

Figure 4 shows the microstructural evolution of 2024 aluminum alloy partially remelted at 620 °C (φ_L=38.8%) for 10−40 min. As shown in Fig. 4(a), after a short holding time, the alloy entirely recrystallizes and the microstructure consists of fine and globular grains with some intergranular liquid. With prolonged holding time, the globules coarsen evidently and become more spheroidal, and the mount of intergranular liquid also increases (Figs. 4(b) and (c)). When the holding time increases to 40 min, the microstructure consists of almost perfectly globular grains, and the intragranular liquid droplets coalesce forming some liquid pools. The liquid content in the micrograph is less in comparison with that obtained from the DSC result shown in Fig. 1, which is attributed to the solidification of liquid into the solid particles during the transferring and quenching from furnace to water. Coalescence between adjacent grains occurs, leading to the formation of large grains with irregular shapes, as indicated by the red rectangles in Fig. 4(c); with prolonging the holding time, some adjacent grains are unified by coalescence, as indicated by the red rectangles in Fig. 4(d). Some small spheroidal grains were detected in the liquid-rich regions, as indicated by the red circles in Figs. 4 (c) and (d).

Figure 5 shows the grain size and shape factor of as-received 2024 aluminum alloy during partial remelting at 620 °C for different holding time. As shown in Fig. 5, with prolonging the holding time, the grain size increases continuously, and the grains tend to be increasingly globular. When the soaking time increases from 10 to 40 min, the grain size increases from an average of ~45 to ~90 μm. The shape factor of solid grains is 0.84 with holding time of 40 min.

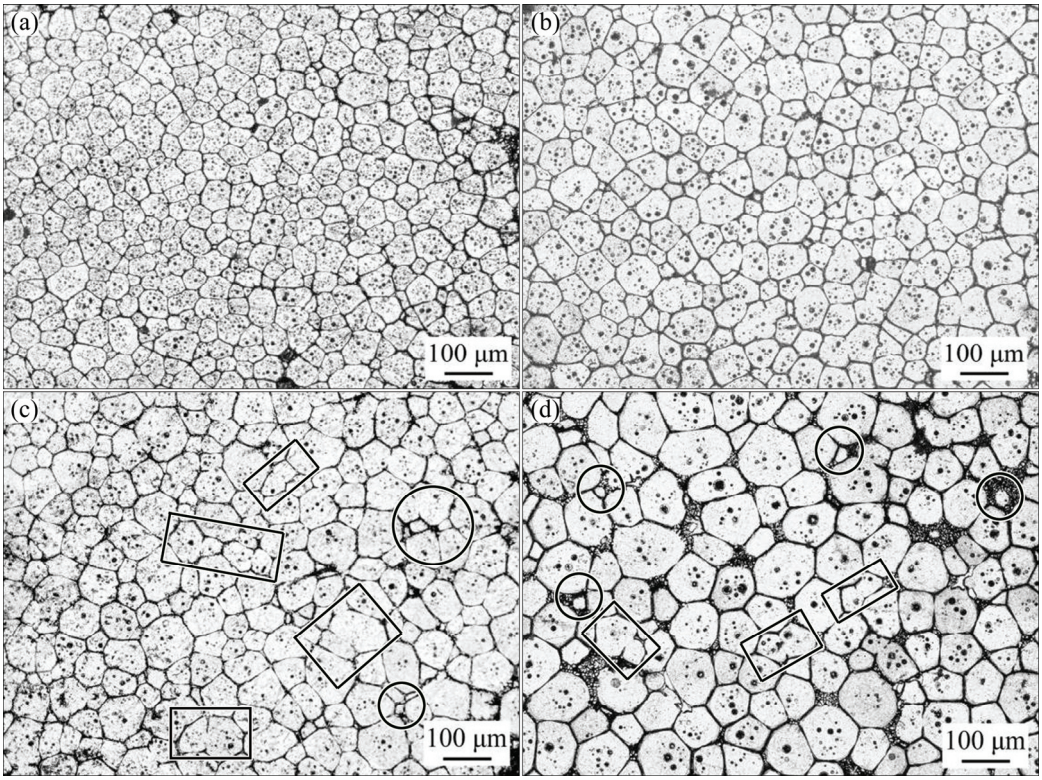

Fig. 4 Microstructures of 2024 aluminum alloy after isothermally holding at 620 °C for 10 min (a), 20 min (b), 30 min (c) and 40 min (d)

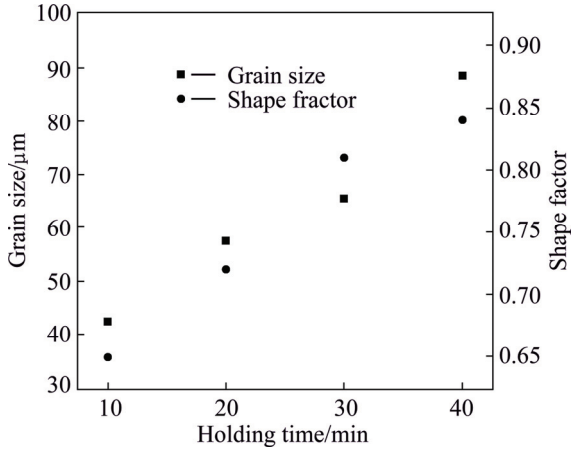

Fig. 5 Grain size and shape factor of 2024 aluminum alloy partially melted at 620 °C for different holding time

3.2 Microstructures of indirectly thixoformed 2024 aluminum alloy

Figure 6 shows the microstructures in different positions of the thixoformed component at a specific pressure of 250 MPa, and the thickness of base is 3 mm. Positions 1 to 4 are located in columns 1 to 4 with decreasing volume, and Position 5 is in the base. As shown in Fig. 6, the microstructures exhibit notable difference among different positions, indicating that obvious segregation occurs during the thixoforming process. In Positions 1 and 2, the solid grains almost remain spheroidal without any plastic deformation, and the liquid phase represented by the intergranular fine dendritic cells seems to segregate under the forming pressure (Figs. 6(a) and (b)). Besides, some micro-porosities were detected in Position 1 (indicated by the red circles in Fig. 6(a)), which could heavily degrade the mechanical properties. As shown in Figs. 6(c) and (d), the solid grains in Positions 3 and 4 are deformed slightly, and the amount of intergranular liquid phase is much less than that in Positions 1 and 2. As shown in Fig. 6(d), the microstructure in Position 5 entirely consists of fine recrystallized grains, indicating that this region underwent severe plastic deformation which led to dynamic recrystallization during the thixoforming process. There is a striking feature that solid−liquid segregation becomes more obvious when the volume of columns increases (4→3→2→1).

Figure 7 shows the microstructures in different positions of the thixoformed component at a specific pressure of 500 MPa, and the thickness of base is 3 mm. As shown in Fig. 7, the microstructures are similar to those thixoformed at a much lower pressure (250 MPa) shown in Fig. 6. There are still some micro-porosities in Position 1 (indicated by red circles in Fig. 7(a)), where the grains also remain spheroidal without any plastic deformation. Theoretically, the solidification defects such as micro-porosities and segregation can be

Fig. 6 Microstructures of thixoformed component in different positions (specific pressure of 250 MPa and base thickness of 3 mm): (a) Position 1; (b) Position 2; (c) Position 3; (d) Position 4; (e) Position 5

eliminated at high forming pressure, and the homogeneity of microstructures can also be improved. However, although the specific pressure increases from 250 to 500 MPa, the four columns do not receive the positive effect by increasing the forming pressure.

Figure 8 shows the grain size and shape factor in different regions. Components 1 and 2 were thixoformed at 250 and 500 MPa, respectively. As shown in Fig. 8 (a), the grain sizes in four regions are all larger than the initial values before the thixoforming, and are very similar between two components. As shown in Fig. 8(b), although the shape factors in four regions are all lower than the initial values, they are still at high values (~0.8 in Positions 1 and 2, ~0.7 in Positions 3 and 4). This indicates that the solid grains in columns did not undergo enough plastic deformation. As the volume of columns decreases (1→2→3→4), the shape factor decreases, indicating that the plastic deformation ratio is larger in smaller columns.

Figure 9 shows the SEM images in Position 1 of Component 2. As shown in Fig. 9(a), a large shrinkage hole was detected between solid grains, as indicated by the red circle. Besides, some solid grains near the hole are separated, as indicated by the red arrows. As shown in Fig. 9(b), some globular grains are surrounded by a large number of fine dendritic cells which were solidified from the liquid phase, indicating that the liquid content in this region is much higher than the normal value due to liquid segregation. Besides, an insoluble particle was detected in the liquid region, as indicated by the red arrow in Fig. 9(b).

Figure 10 shows the SEM image and EDS patterns in Position 1 of Component 2. As shown in Fig. 10(a), coarse eutectic structures form network at grain boundaries, which could heavily degrade the mechanical properties. As shown in Fig. 10(b), the white phase is

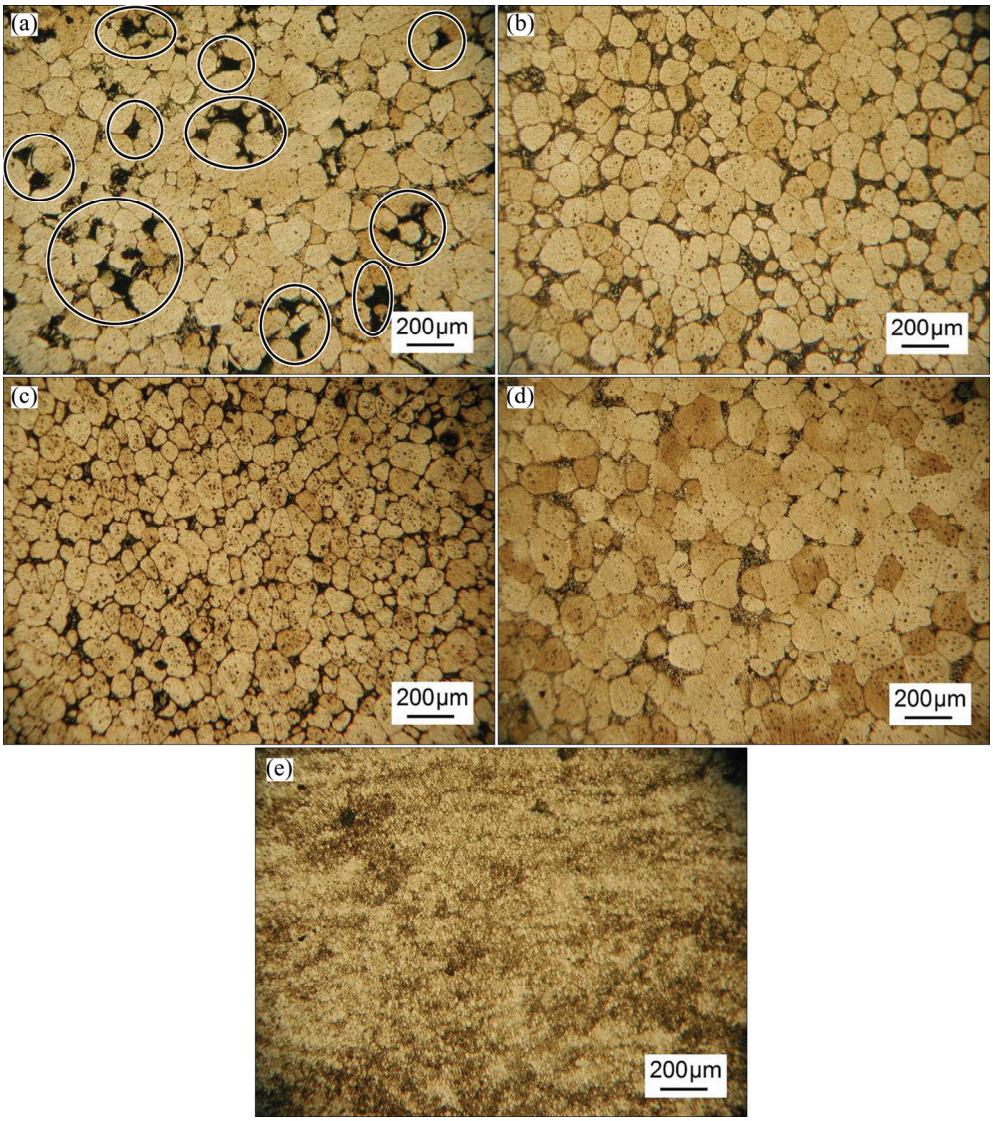

Fig. 7 Microstructures of thixoformed component in different positions (specific pressure of 500 MPa and base thickness of 3 mm): (a) Position 1; (b) Position 2; (c) Position 3; (d) Position 4; (e) Position 5

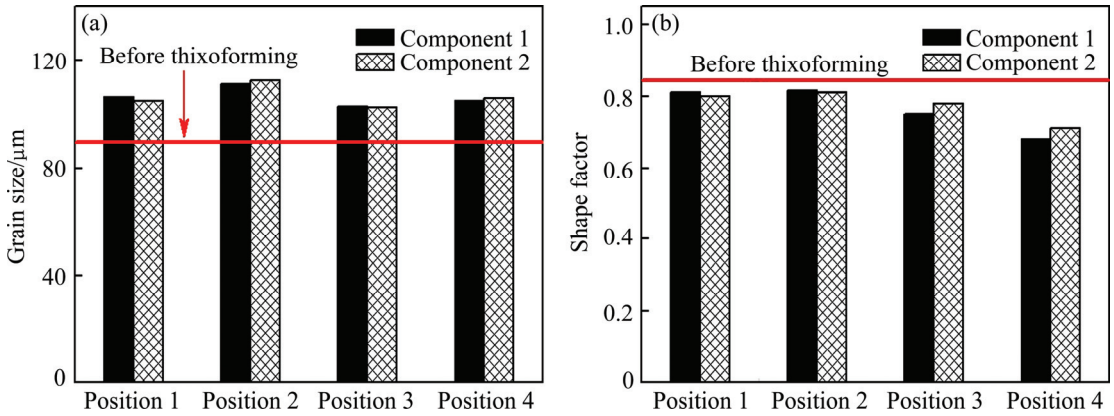

Fig. 8 Grain size (a) and shape factor (b) of thixoformed components in different positions

identified to be Al_2Cu, although the mole ratio of Al to Cu (71.66/24.06) is higher than the stoichiometric value (2/1). The excessive Al content in the spectrum can be attributed to the influence of α(Al) solid solution matrix. As shown in Fig. 10 (c), the content of Cu is 31.54% (mass fraction) in the grey phase, which is close to the eutectic composition (33.2%) of Al−Cu alloy. Therefore, the grey phase should be the eutectic structure

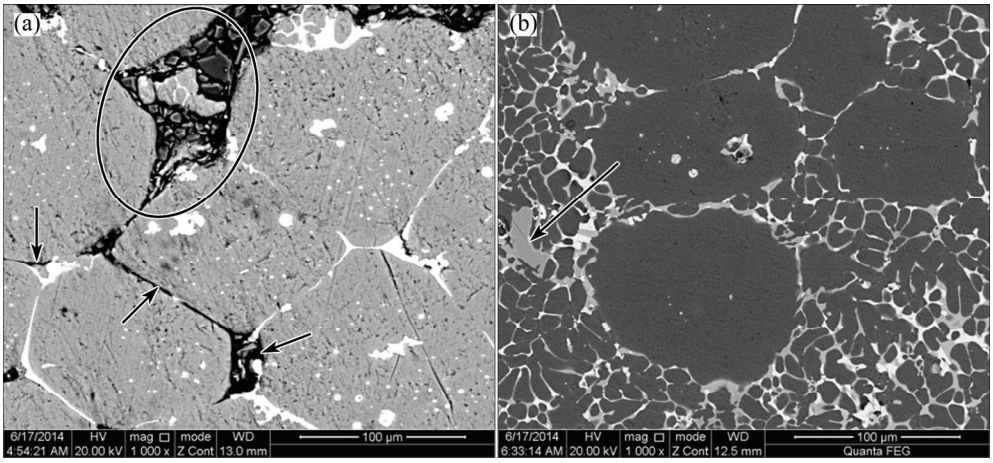

Fig. 9 SEM images of area near porosities (a), and solid−liquid segregation region (b) (specific pressure of 500 MPa and base thickness of 3 mm)

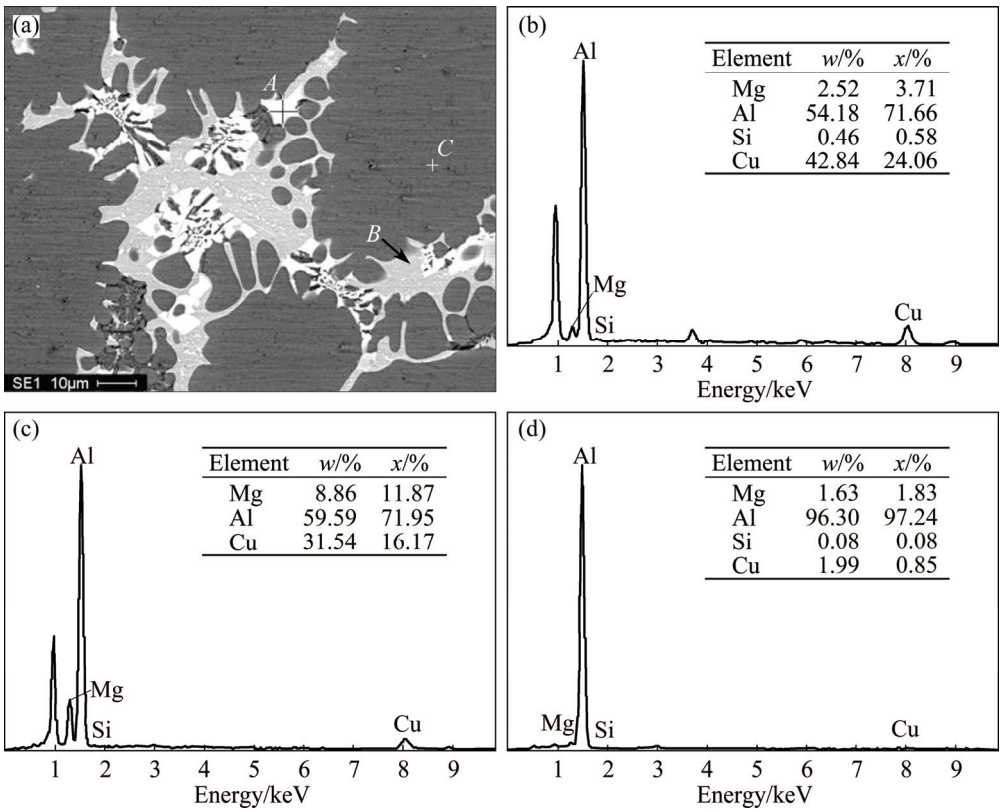

Fig. 10 SEM image of Position 1 (a), EDS patterns of point *A* (b), point *B* (c) and point *C* (d) (specific pressure of 500 MPa and base thickness of 3 mm)

(α(Al)+Al_2Cu). As shown in Fig. 10(d), small amount of Mg and Cu elements exist in the α(Al) matrix. As indicated by the EDS patterns of the three points, the segregation in alloying elements is evident in the thixoformed microstructures.

Figure 11 shows the microstructures in different regions of the thixoformed component at a specific pressure of 500 MPa, and the thickness of base is 10 mm. There is a striking feature in Fig. 11 that, the microstructures of column regions are completely different from those in Figs. 6 and 7. The solid grains in Positions 1 and 2 are deformed evidently (Figs. 11(a) and (b)). Positions 3 and 4 seem to undergo severe plastic deformation, and some dynamic recrystallized grains exist in these regions (Figs. 11(c) and (d)). Whereas, there are still some polygonal grains in base region (Fig. 11(e)), indicating that the deformation in this region is less than that of the component with the base thickness of 3 mm (Fig. 7(e)). As indicated in Fig. 11, the microstructures are almost homogeneous among

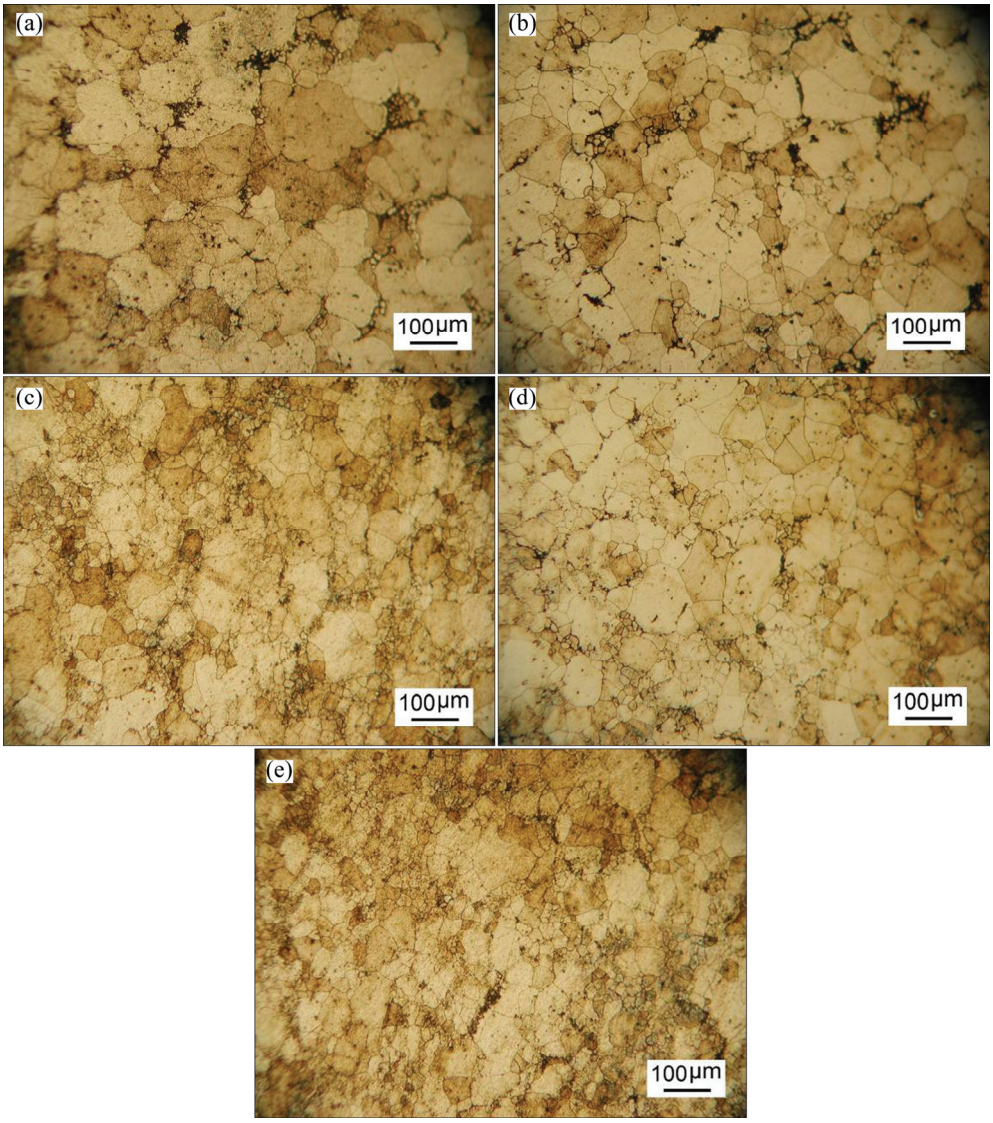

Fig. 11 Microstructures of thixoformed component in different positions (specific pressure of 500 MPa and base thickness of 10 mm): (a) Position 1; (b) Position 2; (c) Position 3; (d) Position 4; (e) Position 5

different regions. Moreover, in comparison with Figs. 6 and 7, the segregation in the four columns is almost eliminated in the component with base thickness of 10 mm.

Figure 12 shows the tensile mechanical properties of thixoformed components at different positions. For Components 1, 2, and 3, the forming specific pressures are 250, 500 and 500 MPa, and the base thicknesses are 3, 3 and 10 mm, respectively. The main purpose of this work is to study the segregation behavior, so the thixoformed components were designed to obtain district solid−liquid segregation phenomenon, not excellent mechanical properties. As a result, the tensile mechanical properties are not very high. As shown in Fig. 12, the ultimate tensile strength (UTS), yield strength (YS) and elongation to fracture of Component 1 are very close to those of Component 2, indicating that the increase of applied pressure from 250 to 500 MPa has little positive effect on the tensile mechanical properties. However, the UTS, YS and elongation to fracture of Component 3 have significant improvement over those of Components 1 and 2 in the four columns. For all components, the UTS, YS and elongation to fracture all increase from Position 1 to Position 5, which are the highest in the base region. However, the difference of mechanical properties among different regions is relatively little in Component 3, while Components 1 and 2 exhibit obvious inhomogeneity in the mechanical properties among different regions.

4 Discussion

4.1 Microstructure evolution during partial remelting

The as-received 2024 aluminum alloy was supplied in extruded state, and underwent severe plastic deformation, as shown in Fig. 3. Severe deformation

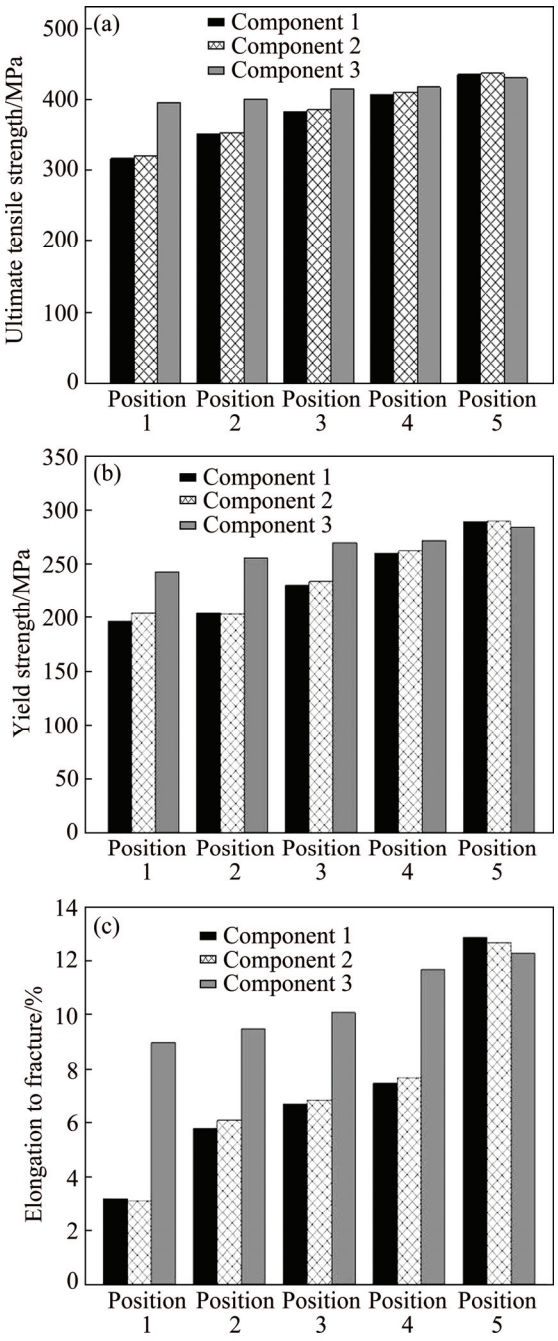

Fig. 12 Tensile mechanical properties of thixoformed components at different positions: (a) Ultimate tensile strength; (b) Yield strength; (c) Elongation to fracture

results in the distortion of crystal lattices and the accumulation of dislocations in the deformed grains, hence leading to large accumulation of distortion energy in the as-received 2024 alloy. Besides, a large number of grains and sub-grain boundaries were generated due to severe plastic deformation. As the temperature increases during the partial remelting, recrystallization occurs in the extruded alloy, and when the liquid forms at temperatures above the solidus, it wets the recrystallized grains. Then, the grain coarsening and spheroidization are activated simultaneously in order to reduce the system energy. The solid grain coarsening mainly follows two types: coalescence and Ostwald ripening [21]. Coalescence occurs by boundary migration when the adjacent grains share a common crystallographic orientation, as indicated by the red rectangles in Fig. 4. Ostwald ripening occurs due to the concentration gradient between solid particles with different sizes in the liquid matrix, which results in large grains growing at the expense of small ones, as indicated by the red circles in Fig. 4. Grain growth by coalescence is dominant at short time after liquid forms with low liquid fractions, while Ostwald ripening is dominant at longer holding time and high liquid fractions. Therefore, when the alloy is isothermally held for 30 min, coalescence occurs between adjacent grains; with prolonging the holding time to 40 min, some grains become unified and grain coarsening is mainly controlled by Ostwald ripening.

4.2 Segregation behavior under different mechanical conditions

The semi-solid structure consists of solid grains and intergranular liquid matrix, and the fluidity of liquid is much better than that of the solid grains. The schematic distribution of solid grains and liquid matrix of the component is shown in Fig. 13, which is consistent with the microstructure distribution in different regions. For indirect thixoforming, the punch moved upward to force the slug into the previously closed die and thixoform it to the desired component. The applied pressure was transferred to the columns by thixotropic flowing and plastic deformation of semi-solid alloy in the center base region. During the thixoforming process, the solid grains and liquid phase can hardly move with a similar velocity. Therefore, most of liquid phase incorporated with some solid grains were firstly squeezed into the columns (Positions 1, 2, 3 and 4) leaving behind a full solid region (Position 5), as shown in Fig. 6. As a result, the segregation between solid and liquid phases is caused in the thixoformed components. The largest two columns (1 and 2) contain most of liquid phase, while the base region behaves as full solid materials with high resistance to deformation. Besides, some micro-porosities will be caused in Position 1 (the final solidification position) under the adverse effect of

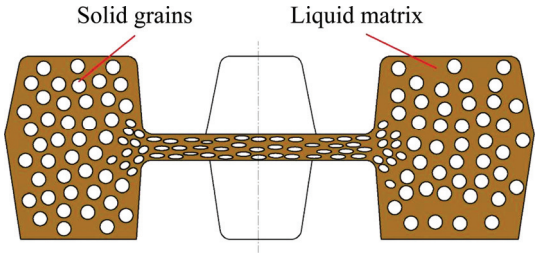

Fig. 13 Schematic diagram of distribution of solid particles and liquid phase

solidification shrinkage. Moreover, the segregation will be more serious in the wrought aluminum alloys which have inferior fluidity in the semi-solid state.

As summarized by CHEN and TSAO [22], there are four mechanisms controlling the deformation of alloys in the semi-solid state: the liquid flow (LF) mechanism and the flow of liquid incorporating solid particles (FLSs) mechanism when the solid particles are surrounded by the liquid phase (high fraction of liquid); the sliding between solid particles (SSs) mechanism and the plastic deformation of solid particles (PDSs) mechanism when the solid particles contact with each other (low fraction of liquid). For this work, the distribution of the dominance of each mechanism is shown in Fig. 14.

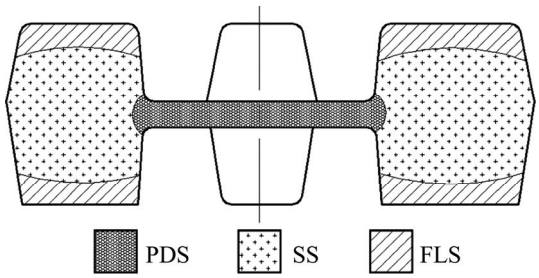

Fig. 14 Schematic diagram of distribution of deformation mechanism during thixoforming

As shown in Fig. 14, the deformation of base region is controlled by the PDSs mechanism. Therefore, the base region is too thin and difficult to be deformed along the loading direction, when the thickness of base is 3 mm. During thixoforming, the base region endures almost all pressure applied by the punch. The pressure can be hardly transferred to the columns (where there is much liquid phase, and the semi-solid alloy does not solidified completely) via the plastic deformation of base region. Therefore, although the specific pressure increases from 250 to 500 MPa, the segregation is not eliminated, and there are still some micro-porosities in the largest column (Fig. 7).

For bulk metal forming, the materials are more easily deformed in the direction where the dimension is larger. When the base thickness increases to 10 mm, it can be compressed plastically along the normal direction due to larger thickness. Therefore, the pressure applied by the punch can be transferred to the column regions by the plastic flow of the base materials, and the semi-solid alloy is in three-dimensional compression stress state. The defects such as micro-porosities can be avoided, and the segregation can also be eliminated under the favorable mechanical condition (Fig. 11).

The tensile mechanical properties of thixoformed components are consistent with the microstructures. The ultimate tensile strength (UTS), yield strength (YS) and elongation to fracture of column regions are all improved significantly under favorable mechanical condition in Component 3 (Fig. 12). The micro-porosities and liquid segregation can adversely affect the mechanical properties of Components 1 and 2, and the elongation to fracture is degraded most. When the semi-solid alloy undergoes high applied pressure due to favorable mechanical condition, the defects such as micro-porosities and liquid segregation can be eliminated. Therefore, high and uniform mechanical properties are obtained in Component 3. The UTS, YS and elongation to fracture in the base region of Component 3 decrease slightly compared with those of Components 1 and 2. This is attributed to that the deformation ratio is larger in the thinner base region, which leads to greater strain-hardening effect.

4.3 Improvement in mechanical condition during thixoforming process

During indirect thixoforming, the mechanical condition has important effect on the microstructures and mechanical properties, and it has also been indicated in the previous work for direct thixoforming [23]. In this work, favorable mechanical condition can be obtained by increasing the thickness of base region. For indirect thixoforming, the role of base region is a gate for materials flowing into the die. Figure 15 shows the schematic diagram of improvement in mechanical condition by applying a secondary pressure in the thixoforming process. As shown in Fig. 15, when the semi-solid alloy fills the die under the pressure applied by the prime punch, secondary pressure is then applied on the column regions by assisted punch. Therefore, the semi-solid alloy will be in three-dimensional compression stress state, and the defects such as micro-porosities and liquid segregation can be avoided under a favorable mechanical condition.

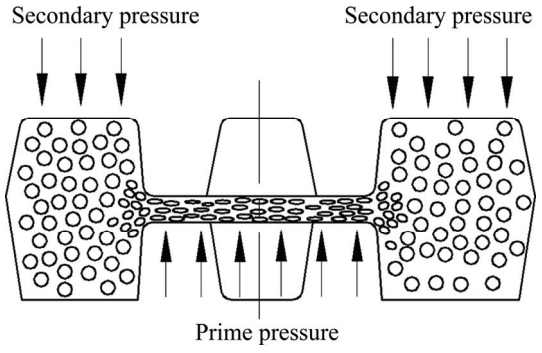

Fig. 15 Schematic diagram of improvement in mechanical condition by applying secondary pressure

5 Conclusions

1) With prolonged holding time during partial

remelting, the solid grains of 2024 aluminum alloy coarsen evidently and become more spheroidal. When the soaking time increases from 10 to 40 min, the grain size increases from an average of ~43 to ~90 μm, and the shape factor increases from 0.65 to 0.84. The microstructure coarsening of the RAP alloy follows two types: coalescence at low liquid fractions and Ostwald ripening when more liquid presents with prolonged soaking time.

2) The thixoformed component reveals a sound and relatively homogeneous microstructure among different regions, and presents no evidence of liquid segregation and micro-porosities under proper mechanical condition. Under unsuitable mechanical conditions (the columns can hardly obtain enough pressure applied by the punch when the base thickness is 3 mm), the microstructures are inferior and inhomogeneous among different regions, and some defects such as micro-porosities and liquid segregation are detected in columns.

3) The distribution of tensile mechanical properties is consistent with that of microstructures. The ultimate tensile strength (UTS), yield strength (YS) and elongation to fracture are improved significantly under favorable mechanical condition. A technical method for improving the mechanical conditions is proposed, which describes the process that semi-solid alloy fills the die firstly under the effect of prime pressure, and then a secondary pressure was applied on the unsolidified region to eliminate the liquid segregation and micro-porosities.

References

[1] ATKINSON H V. Modelling the semisolid processing of metallic alloys [J]. Progress of Materials Science, 2005, 50(3): 341−412.

[2] CHAYONG S, ATKINSON H V, KAPRANOS P. Thixoforming 7075 aluminium alloys [J]. Materials Science and Engineering A, 2005, 390(1): 3−12.

[3] CHEN Qiang, YUAN Bao-guo, LIN Jun, XIA Xiang-sheng, ZHAO Zu-de, SHU Da-yu. Comparisons of microstructure, thixoformability and mechanical properties of high performance wrought magnesium alloys reheated from the as-cast and extruded states [J]. Journal of Alloys and Compounds, 2014, 584: 63−75.

[4] CHEN Qiang, ZHAO Zu-de, ZHAO Zhi-xiang, HU Chuan-kai, SHU Da-yu. Microstructure development and thixoextrusion of magnesium alloy prepared by repetitive upsetting-extrusion [J]. Journal of Alloys and Compounds, 2011, 509(26): 7303−7315.

[5] ATKINSON H V, BURKE K, VANEETVELD G. Recrystallisation in the semi-solid state in 7075 aluminium alloy [J]. Materials Science and Engineering A, 2008, 490(1): 266−276.

[6] KOEUNE R, PONTHOT J P. A one phase thermomechanical model for the numerical simulation of semi-solid material behavior. Application to thixoforming [J]. International Journal of Plasticity, 2014, 58: 120−153.

[7] CHEN Qiang, LUO Shou-jing, ZHAO Zu-de. Microstructural evolution of previously deformed AZ91D magnesium alloy during partial remelting [J]. Journal of Alloys and Compounds, 2009, 477(1): 726−731.

[8] ZHAO Zu-de, CHEN Qiang, HUANG Shu-hai, CHAO Hong-ying. Microstructural evolution and tensile mechanical properties of thixoforged ZK60-Y magnesium alloys produced by two different routes [J]. Materials and Design, 2010, 31(4): 1906−1916.

[9] CHEN Qiang, YUAN Bao-guo, ZHAO Gao-zhan, SHU Da-yu, HU Chuan-kai, ZHAO Zu-de, ZHAO Zhi-xiang. Microstructural evolution during reheating and tensile mechanical properties of thixoforged AZ91D-RE magnesium alloy prepared by squeeze casting-solid extrusion [J]. Materials Science and Engineering A, 2012, 537: 25−38.

[10] KIM H H, KANG C G. Numerical simulation and experimental study for rheo-forged component using direct and indirect die system [J]. Transactions of Nonferrous Metals Society of China, 2010, 20(9): 1799−1804.

[11] CHAYONG S, ATKINSON H V, KAPRANOS P. Multistep induction heating regimes for thixoforming 7075 aluminum alloy [J]. Materials Science and Technology, 2004, 20(4): 490−496.

[12] BOOSTANI A F, TAHAMTAN S. Effect of a novel thixoforming process on the microstructure and fracture behavior of A356 aluminum alloy [J]. Materials and Design, 2010, 31(8): 3769−3776.

[13] BIROLl Y. Thermomechanical processing of an aluminium casting alloy for thixoforming [J]. Journal of Alloys and Compounds, 2009, 479(1): 113−120.

[14] BOOSTANI A F, TAHAMTAN S. Fracture behavior of thixoformed A356 alloy produced by SIMA process [J]. Journal of Alloys and Compounds, 2009, 481(1): 220−227.

[15] LIU D, ATKINSON H V, KAPRANOS P, JIRATTITICHAROEAN W, JONES H. Microstructural evolution and tensile mechanical properties of thixoformed high performance aluminium alloys [J]. Materials Science and Engineering A, 2003, 361(1): 213−224.

[16] KIRKWOOD D H, SELLARS C M, ELIAS BOYED L G. Thixotropic materials: European Patent, 0305375 B1 [P]. 1992.

[17] JIANG J F, WANG Y, ATKINSON H V. Microstructural coarsening of 7005 aluminum alloy semisolid billets with high solid fraction [J]. Materials Characterization, 2014, 90: 52−61.

[18] BIROL Y. Comparison of thixoformability of AA6082 reheated from the as-cast and extruded states [J]. Journal of Alloys and Compounds, 2008, 461(1): 132−138.

[19] CHO W G, KANG C G. Mechanical properties and their microstructure evaluation in the thixoforming process of semi-solid aluminum alloys [J]. Journal of Materials Processing Technology, 2000, 105(3): 269−277.

[20] KANG C G, SEO P K, KANG S S. The effect of injection velocity on liquid segregation and mechanical properties in arm part fabricated by semi-solid die casting process [J]. Journal of Materials Processing Technology, 2006, 176(1): 32−40.

[21] FAN D, CHEN S P, CHEN L Q, VOORHEES P W. Phase-field simulation of 2-D Ostwald ripening in the high volume fraction regime [J]. Acta Materialia, 2002, 50(8): 1895−1907.

[22] CHEN C P, TSAO C Y A. Semi-solid deformation of non-dendritic structures—I. Phenomenological behavior [J]. Acta Materialia, 1997, 45(5): 1955−1968.

[23] CHEN G, DU Z M, CHENG Y S. Effect of mechanical conditions on the microstructures and mechanical properties of thixoformed Al−Cu−Si−Mg alloy [J]. Materials and Design, 2012, 35: 774−781.

Al−Cu−Mg−Mn 合金触变成形显微组织演变与偏析行为

陈 刚[1]，周 焘[2]，王 博[3]，刘洪伟[1]，韩 飞[1]

1. 哈尔滨工业大学(威海) 材料科学与工程学院，威海 264209；
2. 空军装备部 重点型号部，北京 100081；
3. 北京卫星制造厂，北京 100094

摘 要：采用再结晶与重熔法(RAP)制备一种 Al−Cu−Mg−Mn 合金(2024)半固态坯料，研究间接触变成形过程中的显微组织演变和偏析行为。结果表明：对商用挤压态 2024 铝合金进行二次重熔处理，可以直接得到具有细小球晶组织的半固态坯料。在间接触变成形过程中增加底部区域厚度可以得到更好的应力分布状态。在三向压应力条件下，构件不同区域的显微组织较为均匀，没有发现明显的固液偏析和微观缩孔，而且柱体处的晶粒产生了明显的塑性变形。构件不同位置的力学性能和显微组织呈现出良好的对应关系。此外，还讨论了成形过程中的变形机制分布规律，并且提出了一种优化成形应力分布状态的工艺方法。

关键词：铝合金；半固态；触变成形；偏析；显微组织

(Edited by Mu-lan QIN)